INSTITUTE OF INFORMATION AND COMMUNICATION TECHNOLOGIES
BULGARIAN ACADEMY OF SCIENCES
CYBERNETICS AND INFORMATION TECHNOLOGIES • Volume **25**, No 4
Sofia • 2025 Print ISSN: 1311-9702; Online ISSN: 1314-4081
DOI: 10.2478/cait-2025-0037

Illumination Invariant Face Recognition and Retrieval Using Local Vertical Index Patterns and Integrated Probabilistic Approach

Uma Maheswari V.[1], *Rajanikanth Aluvalu*[2], *G. R. Anil*[3]

[1]*Department of CSE, Chaitanya Bharathi Institute of Technology, Hyderabad, India*
[2]*Symbiosis Institute of Technology, Hyderabad Campus, Symbiosis International (Deemed University), Pune, India*
[3]*Research Engineer, NetElixir digital solutions, Hyderabad, India*
E-mails: umamaheswariv1184@gmail.com rajanikanth.aluvalu@ieee.org anilgrcse@gmail.com

***Abstract*:** *Automatic face recognition is a major ramification in the field of Artificial Intelligence. Local binary patterns are designed, such as LBP, GLBP, VLBP, and more extended variants were introduced, but many challenges, like face recognition in various illumination conditions, pixel intensity variation, noisy threshold function, and lower recognition rate etc., have not been addressed. In this paper, we propose a novel feature extraction approach for illumination-insensitive facial recognition and object recognition, as well as under the various illumination conditions named LVIP* (*Local Vertical Index-based Patterns*). *This pattern helps to extract features under the varying lighting conditions. Eventually, we also proposed a new similarity measure method based on the feature integration of rudimentary measures to retrieve similar images. The proposed method was investigated on datasets such as Multi–PIE, VGG Face2, IJB, ExDark, and proved to perform better results in terms of precision, accuracy, and recognition rate.*

***Keywords*:** *Face recognition, Illumination variation, Feature extraction, Image retrieval, Similarity measures.*

1. Introduction

Face recognition plays a vital role in many of the applications and projects, as the feedback from real scenes is being by. In fact, an effective automatic face recognition or object recognition system is direly needed for real-time applications, such as person/object detection in various lighting conditions helps us find the truth in many scenarios. Facial Expression Analysis (FEA) is being used in many of the automatic applications in the fields of e-Commerce, education, crime analysis, and neuroscience, etc., [1, 2], to analyze the feedback without direct communication. However, the LBP and variants were introduced for face recognition; there are challenges not been addressed, like illumination [44], intensity variation, etc. In recent years, researchers have done great research on facial recognition and object recognition, and it has improved drastically over the last decade. Due to the rigorous evolution of Artificial Intelligence (AI) become the biggest challenge for strong AI

applications to develop robots with autonomous thinking. Facial recognition and expression recognition and retrieval systems have three imperative steps such as feature extraction, face recognition, and classification. Face recognition can be done using the most familiar approaches like Viola zones, Haar cascade, etc., and classification can also be done by either machine learning or deep learning algorithms. Nevertheless, feature extraction is a conciliatory phase to improve the efficiency of the recognition, as it can be extracted either statistically or dynamically.

2. Literature survey

Zhao and Pietikainen [1] proposed a new method for face analysis; VLBP is an extension of the conventional LBP method and extracts the dynamic texture in the temporal domain. Micro-expression recognition has been done based on the color space and dynamic texture histograms in [3]. Tian, Kanade and Cohn [4] developed an automatic system for facial expression analysis based on the permanent and transient facial features such as eyes, mouth, brows, and deepening of furrows around those regions. In [5], an integrated method with LBP and LPQ, along with Gabor features to analyze the facial expressions. LPQ and sparse representation are enhanced in [9]. Pantic and Rothkrantz [7] developed a contour-based feature extractor for FEA at important regions like the eye and mouth. Gabor-based facial recognition analysis with PCA+LBP used for feature extraction and dimensionality reduction [8]. A person-independent expression recognition is proposed by He and Chen [10] based on the improved local binary patterns and Higher Order Singular Value Decomposition (HOSVD). Rivera, Castillo and Chae [11] proposed a local feature vector descriptor called Local Directional Number Pattern (LDNP) encodes the directional information using the Kirsch mask in eight directions. Weighted adopted Convolutional Neural Networks (CNN) is proposed by Wu et al. [12] to retrieve the feature representation and also address the optimization and discrimination among the various expressions. Muhammad et al. [13] proposed a system that used a bandlet transform to extract the sub-bands of the face image. Later, applied CS-LBP on every block and integrated the features to generate the global feature [13, 21]. Yang and Bhanu [14] presented an image representation called EAI (Emotion Avatar Image) that leverages the out-of-plane head rotation. Belhumeur et al. [15] have presented a new approach to localize the facial parts in an image. Irene et al. (2007) introduced a grid-tracking and deformation system to recognize the expression in image sequences, and a multi-class SVM is used for expression classification [16]. Wu and Lin [17] proposed weighted center regression adaptive feature mapping (W-CR-AFM) to transform the distribution of features for facial expression recognition associated with deep learning. Chen, Xing and Wang [18] used a method for facial expression recognition with a deep CNN and edge computing. Choi and Song [20] proposed a 2D Landmark Feature Map (LFM) for recognizing faces and also integrated the CNN and LSTM to improve the efficiency. Huang et al. [22] proposed spatiotemporal LBP for micro-expression recognition and represented the face feature. Benedikt et al. [23] assessed the uniqueness and permanence of the facial actions for biometric applications. Dibeklioğlu and Gevers [25] aimed to estimate taste liking

through facial expressions. Pham et al. [26] proposed a multi-layer perceptron classifier for checking the status of the current classification, whether it is classified reliably or not. Animative facial recognition has been recognized across languages [27]. Hierarchical Bayesian theme models were proposed for multi-pose facial expression recognition [28]. Hsieh, Lai and Chen [29] modified the optical flow algorithm by imposing constraints to compute the displacements and intensity variations. CNN and MTCNN (Multi-Task Cascaded CNN) were employed for expression recognition and face recognition [30]. In addition, adding an extra layer among the existing layers as nonlinear texture filters helps significantly improve the recognition rate [31].
Guo et al. [32] proposed a robust descriptor called Extended Local Binary Patterns on Three Orthogonal Planes (ELBPTOP) for micro expression recognition. Allaert, Bilasco and Djeraba [33] developed a new feature descriptor named Local Motion Patterns (LMP) for facial microexpression recognition. A fuzzy histogram of optical flow-based orientations was proposed in [34] for face recognition [34]. Maheswari, Raju and Reddy [49], Maheswari, Prasad and Raju [50] and Maheswari, Varaprasad and Viswanadharaju [51] designed Local patterns based on the direction for facial image recognition and retrieval. Local textural patterns were presented extensively for image recognition [48]. Mohsin and Alameen [52] introduced a hybrid approach integrated with the Laplacian of Gaussian (LoG) and wavelet transform, as well as the Canny edge detector, for approximation, security, and to reduce computation cost, among other benefits. Jawad Al Dujaili and Jabar Sabat Ahily [53] used Active Appearance Model (AAM), Pseudo Zernike Moments (PZM), and Bio-Inspired Features (BIF) for excavating the features and Support Vector Regression (SVR) and Support Vector Machine (SVM) for the prediction of the range of the age from facial images. Rana et. al [54] offered a hybrid approach "RoBERTa-1D-CNN-BiLSTM" for Aspect-Based Sentiment Analysis (ABSA) and Bidirectional Long Short-Term Memory (BiLSTM) used for classification. Werdiningsih, Puspitasari and Hendradi [55] proposed ASD using a Convolutional Neural Network (CNN) based model like Visual Geometry Group 19 (VGG19) and MobileNetV2 for recognizing the daily activities of children. Encountering all the above various kinds of feature extraction patterns, the proposed method is conceived with the integration of approaches to achieve accuracy.

The conventional LBP was introduced by Ojala, Pietikainen and Maenpaa [35] and it became breakthrough of the textural patterns in the field of texture analysis. It has been proven that LBP and extended versions of LBP an efficient feature descriptors in terms of less computation, simplicity, and discrimination. The operator computes the texture feature by finding the differences among the surrounding pixels (I_s) and the center pixel (I_c) using the Equation (1). Furthermore, encoded the differences with binary values '1' and '0' where the difference is greater than zero (>0) and less than one (<1), respectively, using the Equation (2), and the illustration is shown in Fig. 1.

(1) $$L_{\mathrm{S,R}} = \sum_{i=1}^{s} f\left(I_{\mathrm{s}} - I_{\mathrm{c}}\right) \times 2^{i} \Big|_{\text{where } i=1,\,2,\ldots,8},$$

where S represents Side pixels and R represents Radiouslike whether a pixel is surrounded by one line of pixel layer or two, etc.,

(2) $$f\left(x\right) = \begin{cases} 1 & \text{if} \quad x \geq 0, \\ 0 & \text{otherwise.} \end{cases}$$

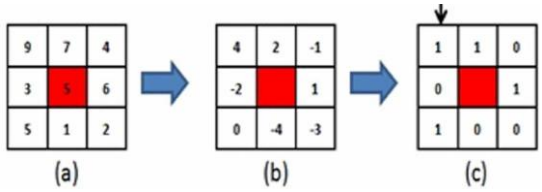

Fig. 1. 3×3 matrix of pixels (a); differences among surrounding pixels and center pixel (b); Substituted with binary encoded values with "1" and "0"; the eight-bit pattern is 11010010 and the decimal equivalent is 210 (c)

3. Proposed method

The confines of the basic LBP, especially the limited range of thresholds, illumination challenges, etc., cannot allow for retrieving the dominant features to fill the gap. Therefore, the operator was already extended to consider the surrounding pixels in various sizes in terms of distance and negative parameters. Examples of extended LBPs are uniform LBP, circular LBP, complete LBP, etc. Among the 2P patterns, uniform LBP considers only those with two numbers of binary transitions.

Here, we adopted the LBP operator to address the problems we are suffering from. As LBP considers only one problem, the negative distance between the pixels cannot be considered. We propose the new patterns. Local Binary Triple Pattern (LBTP) considers the negative values to sharpen the features compared to basic LBP. The basic LBP calculates the differences between surrounding pixels and the centre pixel, which are then converted into the 3-bit binary codes of each difference. In the case of negative values, consider the two's complement of the value. So, eight different values will be encoded into 3-bit binary values at the particular index values. This method addresses the illumination issues, and it confines the edges clearly in all the variations of illumination, particularly in the dusk, as shown in Fig. 2.

The index values of 0-7 bits of every binary value generate a pattern. Similarly, three patterns can be generated as the values were encoded in three bits for eight,

(3) $$I_{\mathrm{d}} = f\left(I_{\mathrm{s}} - I_{\mathrm{center}}\right),$$

(4) $$f\left(x\right) = \begin{cases} \mathrm{DTB}\left(I_{\mathrm{d}}\right) & \text{if} \quad I_{\mathrm{d}} \geq 0, \\ \overline{\mathrm{DTB}\left(I_{\mathrm{d}}\right)} + 1 \text{ if } I_{\mathrm{d}} < 0. \end{cases}$$

Here, $\mathrm{DTB}(I_{\mathrm{d}})$ is the function of converting decimal to binary and $\overline{\mathrm{DTB}(I_{\mathrm{d}})}$ is the 1's complement of the converted binary value.

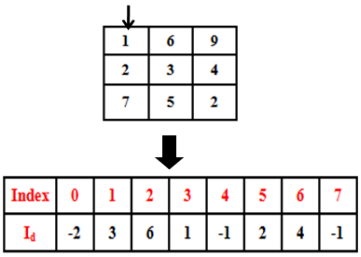

Fig. 2. 3×3-sized pixels and difference values (I_d) of neighborhood and centre pixels, along with index position values

$$\text{DTB}_{3\times 8}\left(I_{\text{d}}\right)=\begin{bmatrix}1 & 0 & 1 & 0 & 1 & 0 & 1 & 1\\ 1 & 1 & 0 & 0 & 1 & 1 & 0 & 1\\ 0 & 1 & 1 & 1 & 1 & 0 & 0 & 1\end{bmatrix}, \tag{5}$$

where DTB represents the Decimal To Binary operation, the above matrix represents the 3-bit binary values using the Equation (4) of the respective differences (I_d) as shown in Fig. 2 (column-wise wise left to right). For example, in Fig. 2, the first difference is –2, as it is a negative difference, it needs to be represented in a 3-bit binary value of 2's complement of 2, i.e., "110" (1's complement of 2 (010) is 101 + 1 = 110) as the Equation (5) depicts. Similarly, remaining values were presented in matrix form as depicted in the Equation (5),

$$\text{Pattern1}=\sum_{i=0}^{p-1}\text{DTB}_{3\times 8}\left(I_{\text{d}}\right)[0,\, j]\times 2^{p}, \tag{6}$$

$$\text{Pattern2}=\sum_{i=0}^{p-1}\text{DTB}_{3\times 8}\left(I_{\text{d}}\right)[1,\, j]\times 2^{p}, \tag{7}$$

$$\text{Pattern3}=\sum_{i=0}^{p-1}\text{DTB}_{3\times 8}\left(I_{\text{d}}\right)[2,\, j]\times 2^{p}, \tag{8}$$

where i represents index positions of pixels like 0-7. And j represents the range of selected index positions.

The above three Equations (6), (7), and (8) were used to generate the three patterns, such as Pattern1, Pattern2, and Pattern3. Furthermore, using the next equation, the average of the three patterns will be computed as

$$\text{LMEBP}_{P,\,R}=\frac{\sum_{p=1}^{3}\text{Pattern}(p)}{3}. \tag{9}$$

Here P represents neighboring pixels, and R represents radius.

Later, the histograms of each pattern can be defined as

$$H_I=\sum_{p,q}I\left(f\left(x,\, y\right)=i\right),\ i=0,1,\ldots,n-1, \tag{10}$$

where n is the number of different labels given by LBP, and p and q are the pixel coordinates in the image,

(11) $$f(m,n)=\begin{cases}1 \text{ if } m=n,\\ 0 \quad \text{else.}\end{cases}$$

The histogram consists of the distributed binary information to extract the spatial information, such as edges, flat areas on faces, marks, etc., in the whole image. Hence, the proposed method generates 3 patterns instead of one in the basic one.

p_1, p_2, p_3 were the histograms enhanced as defined:

(12) $$H_{i,j}=\sum_{p=1}^{3}\sum_{p,q} I\left(f(m,n)=i\right),\ I(m,n)\in p,$$

where p represents the same for the p_1, p_2, and p_3; $H_{i,j}$ represents the gray level i in region j; p and q are pixel coordinates of an image.

In this histogram, the face is represented in three levels of rotation. The labels of the histograms consist of three binary patterns. The histograms were concatenated to produce the global feature vector of the given face image.

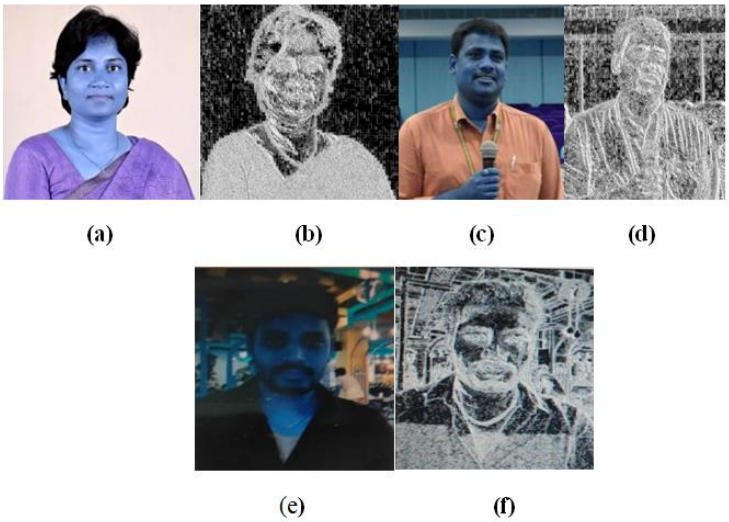

Fig. 3. (a) An image captured with little bright illumination reflected on cheeks, forehead, and neck area so, the feature image (b) retrieves the bright feature more as it is encoded with brighter intensity values. An image labeled (c) has been captured in light dusky illumination (d) shows the feature extracted well where little furrows; facial spatial layout etc. (e) This image captured in full dusk illumination and extracted features very well with content covered by itself for example, Chain on neck is not visible clearly in (e) but it is highlighted with stronger edges and background too. And the shirt color in image (e) is two shaded but it is not recognizable due to less illumination but proposed method works impressive in extracting the color and texture features as well

Algorithm 1

Input: Given image
Output: Feature extracted image

Step 1. Crop the face from the images as part of the preprocessing.
Step 2. Convert the given RGB image into grayscale.

Step 3. Compute the differences of neighbor pixels and center pixel intensity values.

Step 4. Then each of the differences encodes into binary

a. If (I_d >= 0)

Encode the value into binary.

Else

Encode the 2's complement of the value into binary

Step 5. The row indexed (0, 1, and 2) 8 binary values give three 8-bit patterns and find the decimal equivalent value.

Step 6. Later, compute the mean value of 3 patterns to replace the center pixel value and

Step 7. Construct the feature map vector following Step 6.

Step 8. Find the best matches applying the similarity measures as described in Section 5.

Step 9. Retrieve the required image with an expression.

4. Experiments

4.1. Feature-based classification

Clustering / Classification are popular techniques for gaining an understanding of the data's structure through exploratory data analysis. Finding these subgroups in the data is necessary so that data points in the same subgroup are similar and yet differ significantly from those in other clusters. To put it another way, we look for homogeneous clusters within the data, in which each cluster contains data points that are as similar to one another as possible in terms of a similarity metric such as Euclidean-based distance or correlation-based distance. The similarity metric to use is determined by the application. The unsupervised learning methods, such as k-means clustering, SVM, etc., are used when we have unlabeled data and the features extracted from the image based on texture mentioned in Algorithm 1 and shown in Fig. 2. This algorithm's main objective is to classify or organize the data points in a data set. The information is categorized based on its commonalities. k-means attempts to divide the data set into k-clusters using an objective function. SVM classifier also performs well in the recognition of an image based on the feature extracted from the image. Deep learning algorithms such as 2D-CNN, RNN, Auto autoencoders would give better results in image recognition.

4.2. Gaussian kernel

A Gaussian smoothing kernel is used to stabilize photographs. However, using a Gaussian kernel also has the crucial advantage of reducing the impact of noise and shadows on dataset images [47],

$$G(x,y)=\frac{1}{2\pi\sigma^2}e^{-\frac{x^2+y^2}{2\sigma^2}}, \tag{13}$$

where, σ is the standard deviation; using that equation, can calculate the 2D Gaussian filter image, reducing noise.

4.3. Experimental setup and explanation

4.3.1. Multi-PIE

The faces of 337 people were taken in a range of poses, lighting sets, and expressions for the Multi-PIE (Multiple Posed, Illumination, and Expressions) dataset. The position range comprises 15 various perspectives of a face from every angle. Lighting variations were simulated using 19 flashlights scattered throughout the space.

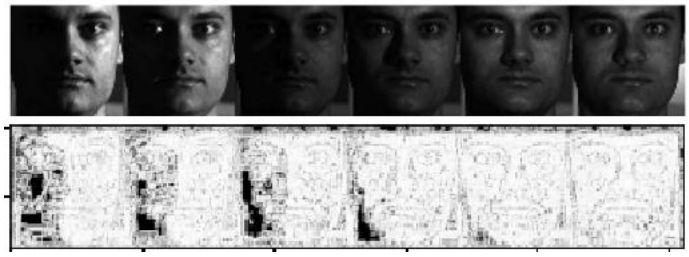

Fig. 4. Multi-PIE sample images and feature images using the proposed method (below)

4.3.2. VGGFace2 Dataset

The collection has 3.31 million photos, with an average of 362.6 for each subject (identity). The collection includes 9131 people. Images from Google Image Search are retrieved, and they exhibit a wide diversity of posture, age, lighting, and races with occupational variations such as actors, politicians, and athletes, etc. The entire dataset is transformed into a training set of 8631 IDs, while the remaining data is transformed into a test set (including 500 identities).

Fig. 5. Sample images of the VGGFace2 Dataset for facial recognition

4.3.3. IARPA Janus Benchmark (IJB)

IARPA Janus Benchmark C (IJB-C), a dataset consisting of photos and video still frames, is used to evaluate face recognition software. In 2017, the collection of 21,294 photographs was made public. Exposing.ai has identified 5757 original images from Flickr that were utilised to build the IJB-C; this information is now searchable using the database search engine on the website. The IJB-C dataset includes photos as well as names. The list includes 3531 names. Among them are

several public speakers, artists, journalists, international politicians, and campaigners. The authors of the IARPA Janus Benchmark-C (IJB-C) dataset used "YouTube users who upload well-labeled, person-centric videos, such as the World Economic Forum and the International University Sports Federation", in contrast to other datasets, such as VGG Face, which began with the Internet Movie Database to collect the names of actors and celebrities. The IJB-C dataset was considered to be the most suitable for these sources.

Fig. 6. Images from the IJB (IARPA Janus Benchmark) dataset were collected from various online sources under various conditions

4.3.4 Exclusively Dark (ExDark) image dataset

The Exclusively Dark (ExDark) dataset encourages more research on finding objects and improving images, especially in low-light settings. The Exclusively Dark (ExDark) dataset consists of 7363 low-light images tagged with 12 object classes, similar to PASCAL Visual Object Classes (PASCAL VOC) on both the image class level and local object bounding boxes. The low-light photographs span from extremely dim settings to dusk in around 10 different conditions. The photographs were taken in a range of lighting conditions, from dusk to very low light.

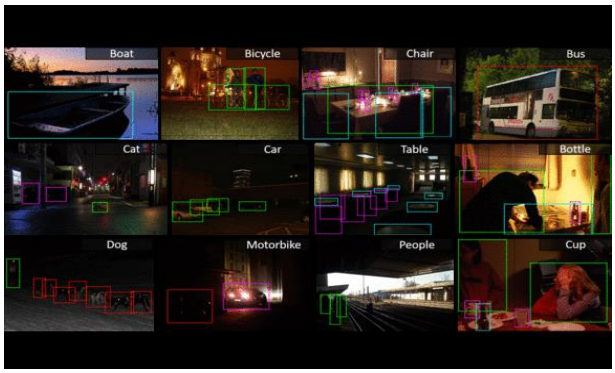

Fig. 7. Sample images of ExDark Image Dataset, which consists of images of various things in dark illumination

5. Similarity measurements

5.1. Minkowski distance

The Minkowski distance is a measurement that applies to normed vector spaces. To compare the separation between two vector points. In addition, the Minkowski distance is frequently utilized in finding the distance between the 2D image pixel coordinate points using the Equation (14).

Let two images query, and the image in the database is assumed to be I_Q and I_{DB},

$$L\left(I_Q, I_{DB}\right) = \left(\sum_{p=0}^{n-1} \left|x_p - y_p\right|^m\right)^{\frac{1}{m}}. \tag{14}$$

Here, p is the pixel points (x_p, y_p) are the coordinate points of image pixels, and m is the real value that can be set to 1 and 2, where $p = 1$ it works as Manhattan distance, $p = 2$ works as the Euclidean distance using the next equation,

$$L\left(I_Q, I_{DB}\right) = \left(\sum_{p=0}^{n-1} \left|x_p - y_p\right|\right), \tag{15}$$

and the Euclidean distance is, it is derived from the Pythagoras Theorem

$$L\left(I_Q, I_{DB}\right) = \left(\sum_{p=0}^{n-1} \left|x_p - y_p\right|^2\right)^{\frac{1}{2}}. \tag{16}$$

5.2. Chi-Square distance

Two feature matrices of images can be compared frequently to determine how similar they are using the chi-square distance statistical formula, using the Equation (17). This distance is generally used in some applications, such as image feature vectors of texture, comparable image retrieval, feature extraction, etc.,

$$\chi^2 = \frac{\sum_{p=0}^{n-1} \left(x_p - y_p\right)^2}{2\left(x_p + y_p\right)}. \tag{17}$$

Here, (x_p, y_p) is the coordinate point of image pixels.

5.3. Canberra distance

This distance is

$$\text{Canberra}\left(I_Q, I_{DB}\right) = \sum_{i=1}^{L} \frac{\left|\text{feature}_{I_{DB,i}} - \text{feature}_{I_{Q,i}}\right|}{\left|\text{feature}_{I_{DB,i}} + \text{feature}_{I_{Q,i}}\right|}, \tag{18}$$

where, I_Q is the image given as query, L is the feature vector length, I_{DB} is the database image.

$\text{feature}_{I_{DB,i}}$ → i-th feature of the database image I_{DB}.

$\text{feature}_{I_{Q,i}}$ → i-th feature of the database image I_Q.

5.4. A novel integrated probabilistic similarity

The concept of integrating the similarity measures is increasing the probability of measuring similarity by combining the features using the Equation (20) of various basic measures, where individual measures are not giving proper results.

Firstly, convert the similarities into probabilities. Let assume the feature as *f* and the subsets of features are designated as $\{f_i\}_{i=0,\ldots,n-1}$ of feature *f*. Similarity measure can be computed with the subset of the feature vector f_i is expressed as follows:

$$S_i = f_i \bullet f_i \to \Re \geq 0. \tag{19}$$

Using the function S_i by using the multiplication of two functions, we obtain the similarity measure of the two images.

According to Bayes' theorem, the probability can be calculated as

$$P\left(H|A_i\right) = \frac{P\left(A_i|H\right)P\left(H\right)}{P\left(A_i\right)}. \tag{20}$$

Here, H stands for homogeneous $P\left(A_i|H\right)$ is the conditional probability density function related to the homogeneous values given by the subset features S_i and $P\left(H|A_i\right)$ is the posterior probability, $P(H)$ is the prior probability that an image is homogeneous, and the $P\left(A_i\right)$ is the unconditional probability where S_i gives a value A_i.

Subsequently, after retrieving the images based on the similarity measures, the output can be computed in terms of precision, accuracy, and recall using the next equations,

$$\mathrm{I}_{\mathrm{Precision}} = \frac{\mathrm{retrieved}}{\mathrm{Total}}, \tag{21}$$

$$\mathrm{I}_{\mathrm{Recall}} = \frac{\mathrm{Number\ of\ relevant\ images\ retrieved}}{\mathrm{Total\ number\ of\ relevant\ images\ in\ DB}}, \tag{22}$$

$$\mathrm{I}_{\mathrm{Accuracy}} = \frac{\mathrm{Total\ number\ of\ right\ predictions}}{\mathrm{Total\ number\ of\ predictions}}. \tag{23}$$

In the Equation (21) total number of predictions includes the correct predictions of True Positive (TP) and True Negative (TN).

Total number of predictions means all right (True) and False predictions of Positive and Negative, i.e., (TP, TN, FP, FN).

Fig. 8 depicts the visible results of the proposed method in finding the images with illumination, especially faces; the proposed model works on the datasets with all cropped images of the aforementioned datasets. Among the dataset images, 20 images were tested for recognition accuracy, as shown in Fig. 8, and 18 images were retrieved based on the similarity measures.

Precision values generated using the various similarity measures and compared with the new method, combined probabilistic features of basic methods such as Minkowski, Euclidean, Canberra, Chi-Square, etc., are shown in Figs. 9-12.

Average image recognition is tested in all the illumination variant images of the various aforementioned datasets. The experimental results are depicted in Fig.13, which shows the observable results on various complex datasets that are created from the real platforms in illumination. Recognition rate is tested on 100 randomly selected images on 6 illumination variations.

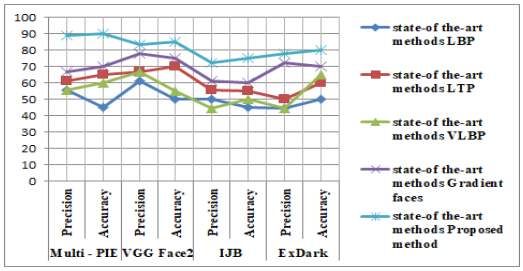

Fig. 8. Precision (Calculated the relevant retrieval images out of 18 images retrieved) and accuracy (tested on 20 random images from the datasets) of the proposed method compared with existing methods LBP, LTP, VLBP, and GradientFaces experimented on various benchmark datasets such as Multi-PIE, VGG Face2, IJB, and ExDark

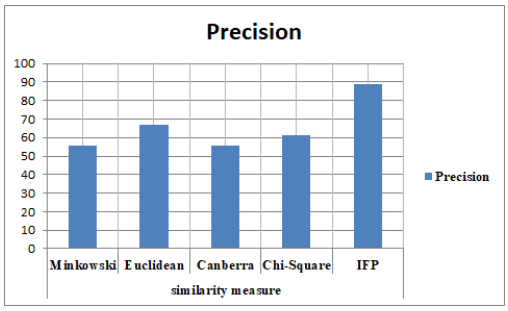

Fig. 9. Precision estimation on the Multi-PIE dataset using various similarity measures compared with novel Integrated Feature Probabilistic (IFP) measure

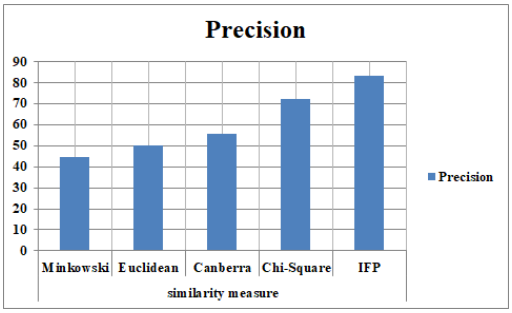

Fig. 10. Precision estimation on the VGG Face2 dataset using various similarity measures compared with the novel Integrated Feature Probabilistic (IFP) measure

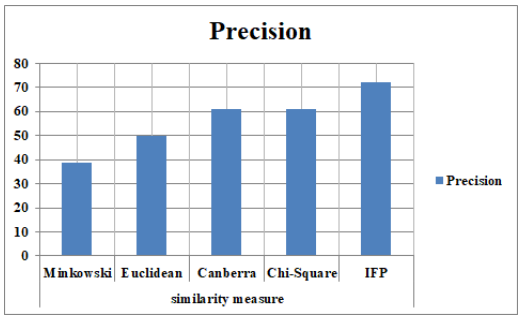

Fig. 11. Precision estimation on the IJB dataset using various similarity measures compared with the novel Integrated Feature Probabilistic (IFP) measure

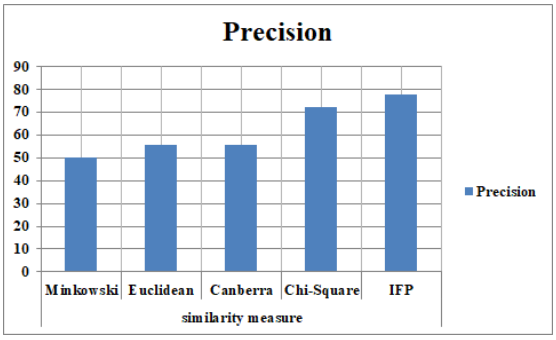

Fig. 12. Precision estimation on the ExDark dataset using various similarity measures compared with the novel IFP Integrated Feature Probabilistic (IFP) measure

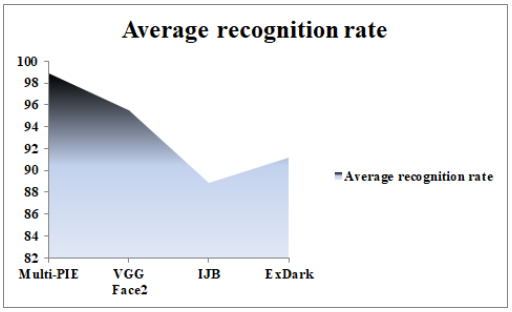

Fig. 13. Average recognition rate of images in different datasets in various illumination conditions

The proposed method can also be used for the classification of images based on the feature vector generated using clustering algorithms such as k-means, SVM, 2D-CNN, etc. This method can be applied directly to any face image or object to extract the feature to recognize. In addition, a Gaussian kernel filter helps much in removing the noise in some kinds of images that have different illuminations causes noise [45, 46].

6. Conclusion

In this correspondence, we proposed a Local Vertical Index-based Patterns (LVIP) to extract the feature to recognize face images and other objects, also under the various illumination conditions. This pattern works well compared to existing approaches that achieve better results in recognizing images in illumination conditions. It has been proven that this approach is effective in overcoming the illumination challenges so far. The proposed method makes differentiation better among the color shades even especially in dark illumination, where the current methods are not working properly. In addition, it is vigorous for various kinds of images taken under different illumination environments. Subsequently, another new approach is also suggested, i.e., integrated probabilistic features as a similarity metric of images in the dataset and test image, instead of basic similarity approaches. The feature can also be used to classify the various illuminated images of objects using machine learning, deep learning, or embedded algorithms to improve the results in terms of recognition.

References

1. Z h a o, G., M. P i e t i k a i n e n. Dynamic Texture Recognition Using Local Binary Patterns with an Application to Facial Expressions. – IEEE Transactions on Pattern Analysis and Machine Intelligence, Vol. **29**, 2007, No 6, pp. 915-928.
2. H u a n g, D., C. S h a n, M. A r d a b i l i a n, Y. W a n g, L. C h e n. Local Binary Patterns and Their Application to Facial Image Analysis: A Survey. – IEEE Transactions on Systems, Man, and Cybernetics, Part C (Applications and Reviews), Vol. **41**, 2011, No 6, pp. 765-781.
3. W a n g, S. J., W. J. Y a n, X. L i, G. Z h a o, C. G. Z h o u, X. F u, M. Y a n g, J. T a o. Micro-Expression Recognition Using Color Spaces. – IEEE Transactions on Image Processing, Vol. **24**, 2015, No 12, pp. 6034-6047.
4. T i a n, Y. I., T. K a n a d e, J. F. C o h n. Recognizing Action Units for Facial Expression Analysis. – IEEE Transactions on Pattern Analysis and Machine Intelligence, Vol. **23**, 2001, No 2, pp. 97-115.
5. Z h a n g, B., G. L i u, G. X i e. Facial Expression Recognition Using LBP and LPQ Based on Gabor Wavelet Transform. – In: 2nd IEEE International Conference on Computer and Communications (ICCC'16), IEEE, October 2016, pp. 365-369.
6. S a u r a v, S., R. S a i n i, S. S i n g h. Facial Expression Recognition Using Dynamic Local Ternary Patterns with Kernel Extreme Learning Machine Classifier. – IEEE Access, Vol. **9**, 2021, pp. 120844-120868.
7. P a n t i c, M., L. J. M. R o t h k r a n t z. Facial Action Recognition for Facial Expression Analysis from Static Face Images. – In: IEEE Transactions on Systems, Man, and Cybernetics, Part B (Cybernetics), Vol. **34**, June 2004, No 3, pp. 1449-1461. DOI: 10.1109/TSMCB.2004.825931.
8. A b d u l r a h m a n, M., T. R. G w a d a b e, F. J. A b d u, A. E l e y a n. Gabor Wavelet Transform-Based Facial Expression Recognition Using PCA and LBP. – In: 22nd IEEE Signal Processing and Communications Applications Conference (SIU'14), April 2014, pp. 2265-2268.
9. W a n g, Z., Z. Y i n g. Facial Expression Recognition Based on Local Phase Quantization and Sparse Representation. – In: 8th IEEE International Conference on Natural Computation, May 2012, pp. 222-225.
10. H e, Y., S. C h e n. Person-Independent Facial Expression Recognition Based on Improved Local Binary Pattern and Higher-Order Singular Value Decomposition. – IEEE Access, Vol. **8**, 2020, pp. 190184-190193.
11. R i v e r a, A. R., J. R. C a s t i l l o, O. O. C h a e. Local Directional Number Pattern for Face Analysis: Face and Expression Recognition. – IEEE Transactions on Image Processing, Vol. **22**, 2012, No 5, pp. 1740-1752.
12. W u, M., W. S u, L. C h e n, Z. L i u, W. C a o, K. H i r o t a. Weight-Adapted Convolution Neural Network for Facial Expression Recognition in Human-Robot Interaction. – IEEE Transactions on Systems, Man, and Cybernetics: Systems, Vol. **51**, 2019, No 3, pp. 1473-1484.
13. M u h a m m a d, G., M. A l s u l a i m a n, S. U. A m i n, A. G h o n e i m, M. F. A l h a m i d. A Facial-Expression Monitoring System for Improved Healthcare in Smart Cities. – IEEE Access, Vol. **5**, 2017, pp. 10871-10881.
14. Y a n g, S., B. B h a n u. Understanding Discrete Facial Expressions in Video Using an Emotion Avatar Image. – IEEE Transactions on Systems, Man, and Cybernetics, Part B (Cybernetics), Vol. **42**, 2012, No 4, pp. 980-992.
15. B e l h u m e u r, P. N., D. W. J a c o b s, D. J. K r i e g m a n, N. K u m a r. Localizing Parts of Faces Using a Consensus of Exemplars. – IEEE Transactions on Pattern Analysis and Machine Intelligence, Vol. **35**, 2013, No 12, pp. 2930-2940.
16. Z h a n g, F., T. Z h a n g, Q. M a o, C. X u. Geometry-Guided Pose-Invariant Facial Expression Recognition. – IEEE Transactions on Image Processing, Vol. **29**, 2020, pp. 4445-4460.
17. W u, B. F., C. H. L i n. Adaptive Feature Mapping for Customizing a Deep Learning Based Facial Expression Recognition Model. – IEEE Access, Vol. **6**, 2018, pp. 12451-12461.
18. C h e n, A., H. X i n g, F. W a n g. A Facial Expression Recognition Method Using Deep Convolutional Neural Networks Based on Edge Computing. – IEEE Access, Vol. **8**, 2020, pp. 49741-49751.

19. H a p p y, S. L., P. P a t n a i k, A. R o u t r a y, R. G u h a. The Indian Spontaneous Expression Database for Emotion Recognition. – IEEE Transactions on Affective Computing, Vol. **8**, 2015, No 1, pp. 131-142.
20. C h o i, D. Y., B. C. S o n g. Facial Micro-Expression Recognition Using Two-Dimensional Landmark Feature Maps. – IEEE Access, Vol. **8**, 2020, pp. 121549-121563.
21. M u h a m m a d, G., M. A l s u l a i m a n, S. U. A m i n, A. G h o n e i m, M. F. A l h a m i d. A Facial-Expression Monitoring System for Improved Healthcare in Smart Cities. – IEEE Access, Vol. **5**, 2017, pp. 10871-10881.
22. H u a n g, X., S. J. W a n g, X. L i u, G. Z h a o, X. F e n g, M. P i e t i k ä i n e n. Discriminative Spatiotemporal Local Binary Pattern with Revisited Integral Projection for Spontaneous Facial Micro-Expression Recognition. – IEEE Transactions on Affective Computing, Vol. **10**, 2017, No 1, pp. 32-47.
23. B e n e d i k t, L., D. C o s k e r, P. L. R o s i n, D. M a r s h a l l. Assessing the Uniqueness and Permanence of Facial Actions for Use in Biometric Applications. – IEEE Transactions on Systems, Man, and Cybernetics. Part A: Systems and Humans, Vol. **40**, 2010, No 3, pp. 449-460.
24. M a r t i n e z, B., M. F. V a l s t a r, B. J i a n g, M. P a n t i c. Automatic Analysis of Facial Actions: A Survey. – IEEE Transactions on Affective Computing, Vol. **10**, 2017, No 3, pp. 325-347.
25. D i b e k l i o ğ l u, H., T. G e v e r s. Automatic Estimation of Taste Liking through Facial Expression Dynamics. – IEEE Transactions on Affective Computing, Vol. **11**, 2018, No 1, pp. 151-163.
26. P h a m, T. T. D., S. K i m, Y. L u, S. W. J u n g, C. S. W o n. Facial Action Units-Based Image Retrieval for Facial Expression Recognition. – IEEE Access, Vol. **7**, 2019, pp. 5200-5207.
27. V e r m a, A., L. V. S u b r a m a n i a m, N. R a j p u t, C. N e t i, T. A. F a r u q u i e. Animating Expressive Faces across Languages. – IEEE Transactions on Multimedia, Vol. **6**, 2004, No 6, pp. 791-800.
28. M a o, Q., Q. R a o, Y. Y u, M. D o n g. Hierarchical Bayesian Theme Models for Multipose Facial Expression Recognition. – IEEE Transactions on Multimedia, Vol. **19**, 2016 No 4, pp. 861-873.
29. H s i e h, C. K., S. H. L a i, Y. C. C h e n. Expression-Invariant Face Recognition with Constrained Optical Flow Warping. – IEEE Transactions on Multimedia, Vol. **11**, 2009, No 4, pp. 600-610.
30. Z h o u, N., R. L i a n g, W. S h i. A Lightweight Convolutional Neural Network for Real-Time Facial Expression Detection. – IEEE Access, Vol. **9**, 2020, pp. 5573-5584.
31. W u, T., N. J. B u t k o, P. R u v o l o, J. W h i t e h i l l, M. S. B a r t l e t t, J. R. M o v e l l a n. Multilayer Architectures for Facial Action Unit Recognition. – IEEE Transactions on Systems, Man, and Cybernetics. Part B: Cybernetics, Vol. **42**, 2012, No 4, pp. 1027-1038.
32. G u o, C., J. L i a n g, G. Z h a n, Z. L i u, M. P i e t i k ä i n e n, L. L i u. Extended Local Binary Patterns for Efficient and Robust Spontaneous Facial Micro-Expression Recognition. – IEEE Access, Vol. **7**, 2019, pp. 174517-174530.
33. A l l a e r t, B., I. M. B i l a s c o, C. D j e r a b a. Micro and Macro Facial Expression Recognition Using Advanced Local Motion Patterns. – IEEE Transactions on Affective Computing, 2019.
34. H a p p y, S. L., A. R o u t r a y. Fuzzy Histogram of Optical Flow Orientations for Micro-Expression Recognition. – IEEE Transactions on Affective Computing, Vol. **10**, 2017, No 3, pp. 394-406.
35. O j a l a, T., M. P i e t i k a i n e n, T. M a e n p a a. Multiresolution Gray-Scale and Rotation Invariant Texture Classification with Local Binary Patterns. – IEEE Transactions on Pattern Analysis and Machine Intelligence, Vol. **24**, 2002, No 7, pp. 971-987. DOI:10.1109/TPAMI.2002.1017623.
36. P a n t i c, M., L. L. M. R o t h k r a n t z. Automatic Analysis of Facial Expressions: The State of the Art. – IEEE Trans. Pattern Analysis and Machine Intelligence, Vol. **22**, December 2000, No 12, pp. 1424-1455.
37. F a s e l, B., J. L u e t t i n. Automatic Facial Expression Analysis: A Survey. – Pattern Recognition, Vol. **36**, 2003, pp. 259-275.
38. K a n a d e, T., J. F. C o h n, Y. T i a n. Comprehensive Database for Facial Expression Analysis. – In: Proc. of International Conference Automatic Face and Gesture Recognition, 2000, pp. 46-53.

39. F e n g, X., M. P i e t i k ä i n e n, A. H a d i d. Facial Expression Recognition with Local Binary Patterns and Linear Programming. – Pattern Recognition and Image Analysis, Vol. **15**, 2005, No 2, pp. 546-548.
40. S h a n, C., S. G o n g, P. W. M c O w a n. Robust Facial Expression Recognition Using Local Binary Patterns. – In: Proc. of IEEE International Conference Image Procession, 2005, pp. 370-373.
41. C o h e n, I., N. S e b e, A. G a r g, L. S. C h e n, T. S. H u a n g. Facial Expression Recognition from Video Sequences: Temporal and Static Modeling. – Computer Vision and Image Understanding, Vol. **91**, 2003, pp. 160-187.
42. S a i s a n, P., G. D o r e t t o, Y. N. W u, S. S o a t t o. Dynamic Texture Recognition. – In: Proc. of Conf. Computer Vision and Pattern Recognition, Vol. **2**, 2001, pp. 58-63.
43. C h e t v e r i k o v, D., R. P é t e r i. A Brief Survey of Dynamic Texture Description and Recognition. – In: Proc. of International Conference Computer Recognition Systems, 2005, pp. 17-26.
44. L i, S. Z., R. C h u, S. L i a o, L. Z h a n g. Illumination Invariant Face Recognition Using Near-Infrared Images. – IEEE Transactions on Pattern Analysis and Machine Intelligence, Vol. **29**, 2007, No 4, pp. 627-639.
45. X u, Y., A. K. R o y-C h o w d h u r y. Integrating Motion, Illumination, and Structure in Video Sequences with Applications in Illumination-Invariant Tracking. – IEEE Transactions on Pattern Analysis and Machine Intelligence, Vol. **29**, 2007, No 5, pp. 793-806.
46. Z h a n g, T., Y. Y. T a n g, B. F a n g, Z. S h a n g, X. L i u. Face Recognition under Varying Illumination Using Gradientfaces. – IEEE Transactions on Image Processing, Vol. **18**, 2009, No 11, pp. 2599-2606.
47. C h e n, T., W. Y i n, X. Z h o u, D. C o m a n i c i u, T. S. H u a n g. Total Variation Models for Variable Lighting Face Recognition. – IEEE Trans. Pattern Anal. Mach. Intell., Vol. **28**, September 2006, No 9, pp. 1519-1524.
48. P r a s a d, G. V., S. V. R a j u. A Survey on Local Textural Patterns for Facial Feature Extraction. – International Journal of Computer Vision and Image Processing (IJCVIP), Vol. **8**, 2018, No 2, pp. 1-26.
49. M a h e s w a r i, V. U., S. V. R a j u, K. S. R e d d y. Local Directional Weighted Threshold Patterns (LDWTP) for Facial Expression Recognition. – In: 5th IEEE International Conference on Image Information Processing (ICIIP'19), IEEE, November 2019, pp. 167-170.
50. M a h e s w a r i, V. U., G. V. P r a s a d, S. V. R a j u. Facial Expression Analysis Using Local Directional Stigma Mean Patterns and Convolutional Neural Networks. – International Journal of Knowledge-Based and Intelligent Engineering Systems, Vol. **25**, 2021, No 1, pp. 119-128.
51. M a h e s w a r i, V. U., G. V a r a p r a s a d, S. V i s w a n a d h a r a j u. Local Double-Directional Stride Maximum Patterns for Facial Expression Retrieval. – International Journal of Biometrics, Vol. **14**, 2022, No 3-4, pp. 439-452.
52. M o h s i n, N. A., H. A. A l a m e e n. A Hybrid Method for Payload Enhancement in Image Steganography Based on Edge Area Detection. – Cybernetics and Information Technologies, Vol. **21**, 2021, No 3, pp. 97-107.
53. J a w a d, A. L., M. D u j a i l i, H. J a b a r S a b a t A h i l y. A New Hybrid Model to Predict Human Age Estimation from Face Images Based on Supervised Machine Learning Algorithms. – Cybernetics and Information Technologies, Vol. **23**, 2023, No 2, pp. 20-33.
54. R a n a, M. R. R., A. N a w a z, T. A l i, A. S. A l a t t a s, D. S. A b d E l m i n a a m. Sentiment Analysis of Product Reviews Using Transformer Enhanced 1D-CNN and BiLSTM. – Cybernetics and Information Technologies, Vol. **24**, 2024, No 3, pp. 112-131.
55. W e r d i n i n g s i h, I., I. P u s p i t a s a r i, R. H e n d r a d i. Recognizing Daily Activities of Children with Autism Spectrum Disorder Using a Convolutional Neural Network Based on Image Enhancement. – Cybernetics and Information Technologies, Vol. **25**, 2025, No 1, pp. 78-96.

Received: 30.06.2025, First revision: 09.09.2025, Second revision: 04.10.2025, Accepted: 10.10.2025